CHAPTER XXIV-2

INTERNAL CRANIAL ANATOMY

Antoine BALZEAU

Abstract

The purpose of this study is to describe the internal cranial anatomy of the Spy 1 and Spy 10 fossils. Indeed, imaging methodologies allow 2D and 3D observation and reconstruction of previously unavailable morphological features, as well as their precise description and quantification. This paper provides exhaustive descriptions and detailed metric data for the pneumatisation of the frontal and temporal bones (disposition, extension and volume) and for the cranial vault thickness and its internal composition. These data are compared with the available information for other Neandertal fossils, as well as for other hominid species and anatomically modern Homo sapiens*, in order to discuss the internal characteristics of the Spy 1 and Spy 10 crania and the variation among Neandertals.*

INTRODUCTION

Among the Neandertal remains unearthed at Spy in 1886 are two partial calvaria, Spy 1 and Spy 10. These crania are composed of many fragments with some missing anatomical parts. Just after the discovery, the fragments were assembled in order to reconstitute the general morphology of the crania and filling material was used to complete the missing parts. The skulls are described in detail regarding their external cranial anatomy elsewhere in this monograph (Rougier *et al.*, this volume: chapter XXIV-1). Similarly, we described in another chapter the virtual cleaning of the crania of all non-osseous elements (Balzeau *et al.*, this volume: chapter XXII; Figure 1a and Figure 2a) by means of imaging methodologies and informatics processing. The purpose of this study is to exhaustively describe and quantify the internal anatomy of the Spy 1 and Spy 10 crania.

Imaging methodologies allow 2D and 3D observation and reconstruction of previously unavailable morphological features, as well as their precise description and quantification. Therefore, this paper provides exhaustive descriptions and detailed metric data for the pneumatisation of the frontal and temporal bones and for the cranial vault thickness and its internal composition. These data are compared with the available data for other Neandertal fossils, as well as for other hominid species and anatomically modern *Homo sapiens*. Then, the internal characteristics of the Spy 1 and Spy 10 crania are discussed, as well as the variation and the particularities of Neandertals regarding these features.

MATERIAL AND METHODS

Morphological and quantitative analyses of the pneumatisation of the frontal and temporal bones, as well as of the cranial vault thickness and internal composition, were conducted using computed tomography (CT) data. Spy 1 and 10 were CT scanned with a Siemens Somaton 64 at the Erasmus Hospital (ULB) in Brussels, Belgium. The settings were 0.6 mm-thick slices, with a reconstruction interval of 0.3 mm, 10-23.8 cm field of view, and 0.195-0.465 mm pixel size with a pixel matrix of 512*512 (Semal *et al.*, 2005). Specific CT acquisitions of the temporal bones were made to have a better definition than the datasets of the complete crania. The fossils were CT scanned during the European project called “The Neanderthal Tools” (TNT; e.g. Macchiarelli *et al.*, 2005; Macchiarelli & Weniger, 2006) and the datasets were stored in the NESPOS database (https://www.nespos.org/). The CT data do not show any noticeable artefacts, and the Hounsfield values are within the range covered by the scanner, resulting in the absence

of overflow artefacts. Comparative data derive from previous works and concern original fossils and imaging datasets for anatomically modern *Homo sapiens* and *Homo erectus*, as well as for Neandertal adult individuals (La Chapelle-aux-Saints 1, La Ferrassie 1, La Quina 5 and 27, Krapina 3, 4, 5, 6, 38.1, 38.11, 38.12, 38.13, 38.21, 39.1, 39.13, 39.14, 39.18).

Following previous experience, the CT data were used to extract information concerning pneumatisation (Balzeau *et al.*, 2003, 2005; Balzeau & Grimaud-Hervé, 2006), cranial vault thickness (CVT) and internal composition of the bones (Balzeau, 2006, 2007). CT datasets correspond to a large number of adjacent 2D images which do not allow for retrieval of the repetitive reconstructed CT images (with respect to orientation and slicing spacing) that are needed to describe the complex morphology of the pneumatisation. Therefore, in order to minimise the possible influence of the acquisition parameters on metric analyses and descriptions, pneumatisation was analysed in three dimensions. The calculation of the reconstruction in 3D was based on data obtained using a segmentation protocol adapted to studying fossil hominid morphology. On each CT slice, the boundary between the bone and the air (the pneumatic cells) was identified by manual segmentation. This protocol required using multiple threshold values as a function of variation of temporal bone mineralization. Values were also adjusted when some sediment was present in the cells. These settings permitted us to obtain precise outlines of the whole pneumatisation and then also obtain precise 3D reconstructions.

A specific analytical protocol was developed to overcome the limitations of analysing cranial vault thickness and internal composition (Balzeau, 2006, 2007) by using the mid-sagittal plane on the CT data. The CT data correspond to a set of successive slices defining the whole fossil. Each image crosses the bony structures in various orientations. Thickness quantification can be done where the acquisition is perpendicular to the cranial surface and thickness. The mid-sagittal plane is the only one in the dataset that extends perpendicularly to the cranial thickness on its full extension. On each individual's corresponding slice, the boundary between outer, diploic and inner table, as well as with the surrounding air, was identified by manual segmentation. This procedure consists of measuring the median value (or Half Maximum Height) of the CT value of the two elements, whose interface is to be defined (Spoor *et al.*, 1993; Schwartz *et al.*, 1998).

Manual segmentation has to be made each time the attenuation coefficient of one of the elements varies along the interface. This allows for the accurate identification of the interface between two structures, despite local fluctuation in CT numbers (Balzeau, 2005). Four principal landmarks are defined on the external cranial surface: the sagittal glabella (noted as Gs), the sagittal bregma (Bs), the sagittal lambda (Ls) and the sagittal external occipital protuberance (Os). The internal projection perpendicularly to the endocranial surface of these landmarks is used to delimitate four endocranial chords. These chords are divided into equal segments; Gs-Bs and Bs-Ls are divided into 20 equal segments, Ls-Os is divided into 15, and Os-foramen magnum is divided into five. The thickness is measured at each interval and quantified perpendicularly to the endocranial surface, since this surface has less topographical variations than the external cranial surface. This protocol provides data for the vault thickness and structural layers distribution on 60 landmarks on the whole mid-sagittal plane.

RESULTS

The results are detailed separately for each cranium: Spy 1 (Figure 1), then Spy 10 (Figure 2). The position and the extension of the frontal sinuses, of the temporal bone pneumatisation and information about the thickness of the cranial vault and its internal composition are detailed below.

Spy 1

In the area corresponding to the frontal sinuses, the frontal bone is composed of several fragments; some parts are missing, particularly for the internal cranial surface on the left side. As a result, the frontal sinuses are incompletely preserved and are exposed endocranially. The bony ridge which separates the right and left si-

nus is absent. Some sediment fills the uppermost cell of the right sinus, in its medial part. The frontal sinuses invade the complete glabellar area of the frontal torus and propagate laterally as far as the middle part of the torus on both sides, just laterally to the supraorbital foramen (Figure 1b and 1c). The sinuses, where present, completely fill the torus antero-posteriorly. Finally, cells continue posteriorly to the postorbital sulcus and propagate slightly in the frontal squama, particularly in its medial part. The sinuses are composed of several large cells. However, cells overlap and are not well individualised because of the sinuses' development. Some tiny bony bridges are present on the internal surface of the frontal bone corresponding to the anterior extension of the frontal sinuses. They propagate posteriorly, with a vertical orientation. Cells are better individualised in their uppermost extension because of differential postero-superior propagation in the frontal squama. The left frontal sinus is slightly larger. The incomplete frontal sinuses have a volume of over 20 cm^3 and extend laterally for 79 mm.

In the right temporal bone, pneumatisation is located around the antrum and forms a compact volume (Figure 1d and 1e). Pneumatic cells have a more prominent extension in all directions than for the left temporal bone. Cells are smaller medially and larger laterally. The two largest cells are the most latero-posterior ones. The largest one extends over 1.5 cm vertically. Anteriorly, cells are located all along the posterior wall of the external auditory meatus and continue vertically in the upper part of the petrous, but do not extend anteriorly to the plane of the anterior semi-circular canal. Medially, cells are located above the lateral semi-circular canal, but pneumatisation does not propagate in the petrous apex. The most lateral cells are in the anterior area of the sulcus between the mastoid and the supramastoid crests.

The most superior and posterior extension of the pneumatisation corresponds to the large cell located in the uppermost area of the junction between the petrous and the squamous temporal. Inferiorly, the cells situated in the anterior part of the mastoid process are just under the level of the deepest point of the digastric groove. Pneumatisation has a volume of 4.8 cm^3.

In the left temporal bone, some sediment is present in the internal auditory meatus, the tympanic cavity, and partially fills the antrum. Pneumatisation is principally localised around the antrum (Figure 1f). Small cells propagate at the inferior extension of the pneumatisation, whereas its postero-superior extension is composed of a few very large cells. Anteriorly, cells extend close to the posterior wall of the external auditory meatus while some others are in the upper part of the petrous, just above the centre of the external auditory meatus. Medially, cells are located just above the superior semi-circular canal. Pneumatisation is present in the superior part of the petrous but does not propagate in its apical area. The most lateral cell is at the junction between the uppermost part of the petrous and the squamous temporal. This large cell is also the most superior one. Inferiorly, cells do not extend under the level of the middle of the external auditory meatus, which also corresponds to the inferior extension of the basal turn of the cochlea. The most posterior extension of the pneumatisation also corresponds to the large cell at the junction between the petrosal and the squamous temporal. The unpneumatised areas of the temporal bone, i.e. the complete squamous temporal, the area posterior to the parietal notch and the mastoid apex, principally consist of the diploic layer. Pneumatisation has a volume of 1.1 cm^3.

The cranial vault thickness was quantifiable on nearly all the midsagittal plane, except for the most anterior part of the frontal bone and the inferior half of the nuchal plane (Figure 1g). Moreover, a few values were affected for a small part of the second half of the frontal bone because of the slight erosion of the internal surface. Finally, three measurements were estimated for the posterior part of the parietal bones because of a gap and the presence of plaster. In what concerns the internal composition of the bones, no information was available where the frontal sinuses extend in the analysed plane. Some values were slightly estimated because of the incomplete preservation of the internal table in the second half of the frontal bone. The maximal thickness for the frontal bone corresponds to the measurement at glabella, with a value of 22.2 mm. The CVT decreases regularly in the direction of the bregma and slightly increases at

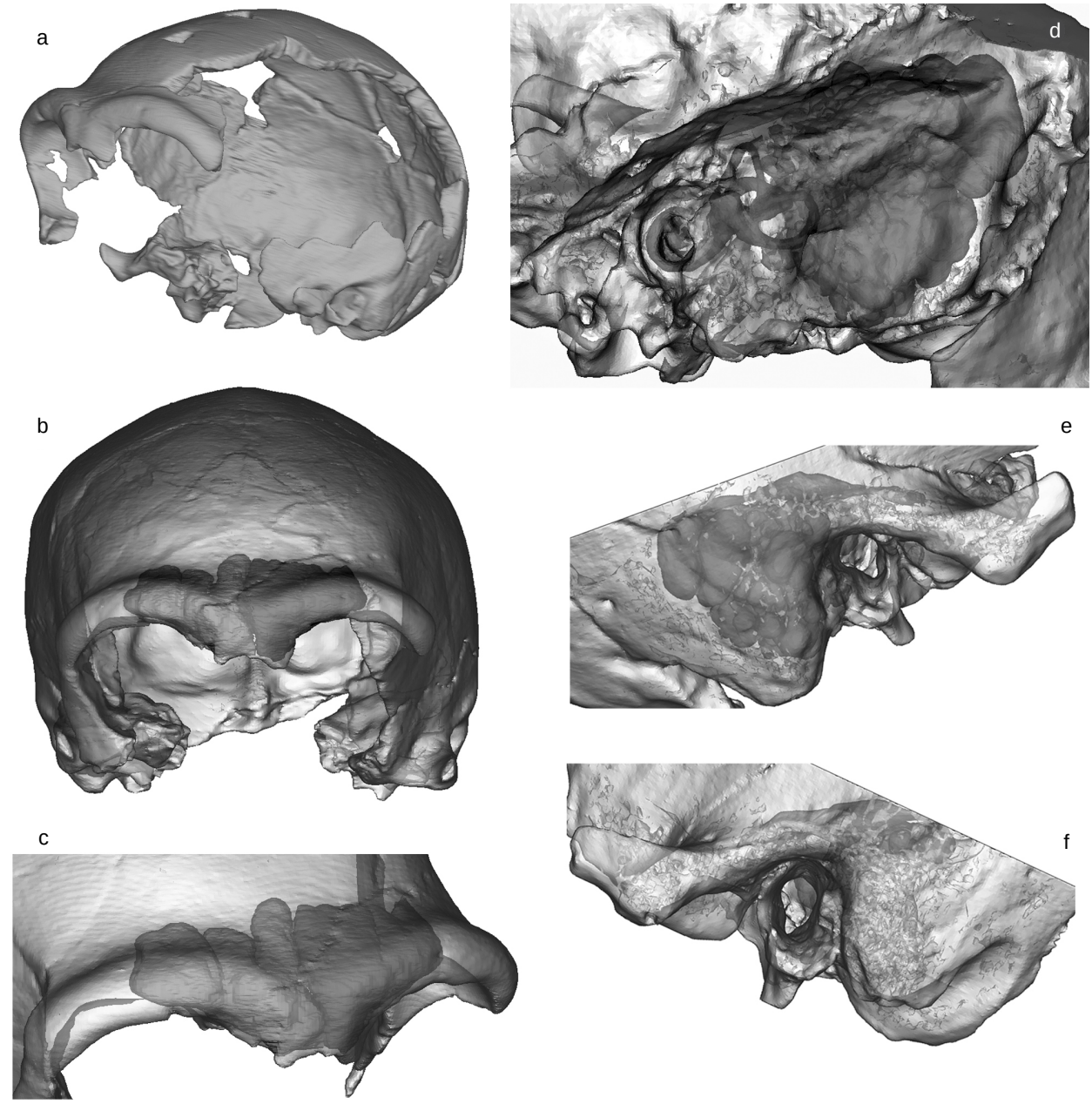
a
b
c
d
e
f
g
(mm)
20
15
10
5
0
Gs
4
8
12
16
Bs
24
28
32
36
Ls
44
48
52
Os
External table
Diploic layer
Internal table

the bregma at 7.4 mm. The thickness at the junction of the parietal bones varies from 7.4 mm in their anterior part, decreases to a minimal value of 6.6 mm in their middle part, and increases as far as the lambda, where it reaches 8.6 mm. There is a thickening in the anterior part of the occipital plane (11.1 mm), and then the thickness decreases in its medial part (10.5 mm) and increases again to reach 14.1 mm as a maximal value where the occipital superstructures are the most developed.

For the internal composition (Figure 1g), the diploic layer constitutes over 56 % of the total thickness in the anterior part of the frontal squama, whereas the internal and external tables both constitute around 22 %. The proportion for the diploic layer decreases in the direction of the bregma, whereas the values for the tabular tables have a regular and similar augmentation. Just anteriorly to the bregma, the internal table represents 34 % of the total thickness, the diploic layer represents 37.6 % and the external table shows 28 %. This variation is due to a variation in the total vault thickness in this area, which only affects the diploic layer. Indeed, absolute values for the tabular tables' thicknesses do not vary to a great extent along the frontal bone. The diploic layer is the principal constituent of the total thickness of the occipital plane. For the area localised above the suprainiac fossa, the diploic layer has a mean representation of 65 % of the total thickness, the external table has a mean of 19 % and the internal table has a mean of 16 %. In the area of the suprainiac fossa, the diploic layer has a thickness of approximately 6.9 mm, the external table is around 2.5 mm, and the internal table is about 2 mm. From just above the suprainiac fossa to the most posterior prominent point of the occipital torus, mean values are 56 % for the diploic layer, 27 % for the external table and 17 % for the internal table. The diploic layer has a thickness of around 7.4 mm, the external table is about 4.2 mm, and the internal table is about 2.5 mm where the occipital superstructures are the most developed.

Figure 1. (opposite page) Internal cranial anatomy of Spy 1: original state of preservation of the fossil (a), 3D reconstructions based on CT data of the fossil and the frontal sinuses in anterior view (b) and right antero-lateral view (c), of the right temporal bone and its pneumatisation in endo-posterior (d) and lateral views (e), of the left temporal bone and its pneumatisation in lateral view (f), and variation in the cranial vault thickness and in the thickness of the inner table, diploe and outer table (in mm) along the mid-sagittal plane (g).

Spy 10

The frontal bone is complete, except for its lateral parts at the junction with the right parietal and temporal bones and with the left temporal bone, and except for the medial part of the frontal torus. As a result, a large part of the original extension of the frontal sinuses cannot be described. The sinuses probably completely filled the glabellar region based on their lateral extension (Figure 2b). On the right side, the sinus continues laterally to the supraorbital foramen, which is not preserved. So, this cavity is included in the area of the torus where its thickness is maximal vertically, and does not propagate in the lateral area, where the torus becomes thinner. The sinus has a weaker lateral extension on the left side and does not reach the level of the supraorbital foramen.

The frontal sinuses were most certainly contained inside the frontal torus, based on the actual state of conservation of the frontal squama in its broken medial part, and the absence of bony walls corresponding to the surface of the sinuses. A very small cell on the left side has a slight posterior propagation in the area of the postorbital sulcus. On the right side, the lateral extension of the sinus is constituted by a large cell, separated medially from another large cell by two bony walls and a smaller sinusal cavity. Below and posterior to this lateral cell, another one is well individualised and has an elongated shape. The right sinus is larger. It is not possible to estimate the volume of the frontal sinuses because of their incomplete preservation. They extend laterally for 66 mm.

The right temporal bone is complete, except for the anterior part of the squamous and the basal and posterior areas of the petrous. Pneumatic cells are partially broken and exposed in this area, as well as in the summit of the posterior wall of the petrous.

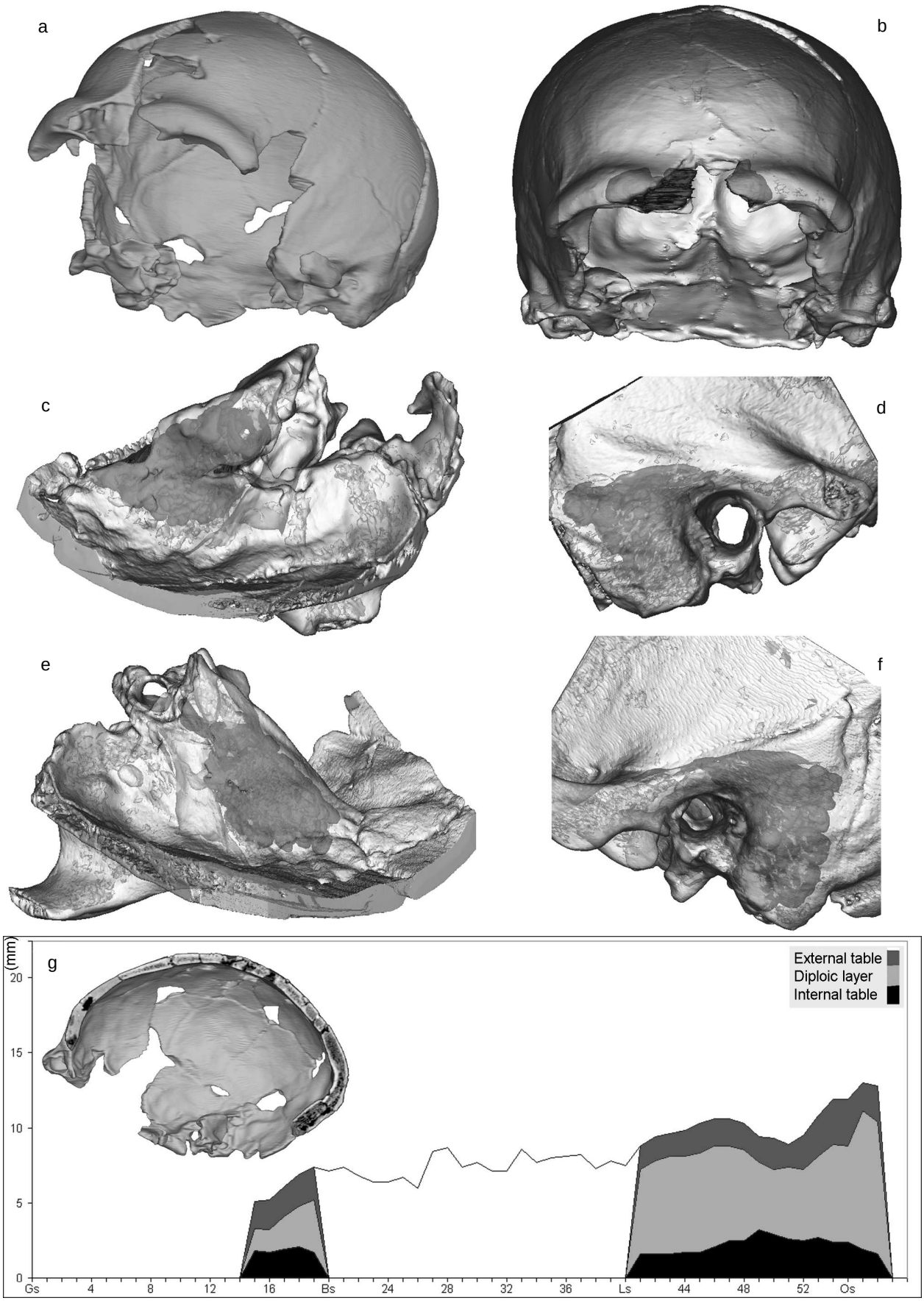
a
b
c
d
e
f
g
External table
Diploic layer
Internal table
(mm)
20
15
10
5
0
Gs
4
8
12
16
Bs
24
28
32
36
Ls
44
48
52
Os

Pneumatisation constitutes a compact volume in the petromastoid area (Figure 2c and 2d). Anteriorly, cells extend all along the posterior surface of the external auditory meatus. Medially, cells are situated above the lateral semi-circular canal and propagate posteriorly to the bony labyrinth as far as the plane of the superior semi-circular canal, but do not continue farther in the petrous apex. The most lateral cells are in the anterior area of the sulcus between the mastoid and the supramastoid crests.

Superiorly, pneumatisation reaches the level of the summit of the superior semi-circular canal. The more inferiorly located cells are in the basal part of the posterior wall of the petrous. Based on their position and the actual state of preservation of the temporal bone, pneumatisation probably did not propagate inferiorly to the deepest point of the digastric groove. Moreover, cells are absent in the mastoid process. The most posterior cell is located at the uppermost portion of the junction between the petrosal and the squamous temporal. This cell is exposed because of the incompleteness of the posterior wall of the petrosal. Pneumatisation constitutes a volume of 2.5 cm^3, but this value is underestimated.

The left temporal bone is complete, except for the petrous apex and the postero-inferior part of the petrous, medially to the digastric groove. In this last area, some pneumatic cells are exposed. The tympanic cavity is partially preserved. Pneumatisation constitutes a compact volume in the petromastoid area (Figure 2e and 2f). Anteriorly, cells extend along the posterior wall of the external auditory meatus. The most anterior cells are just below the lateral extension of the antrum. Medially, cells are located above the lateral semi-circular canal, just below the summit of the posterior canal.

Figure 2. (opposite page) Internal cranial anatomy of Spy 10: original state of preservation of the fossil (a), 3D reconstructions based on CT data of the fossil and the frontal sinuses in anterior view (b), of the right temporal bone and its pneumatisation in superior (c) and lateral views (d), of the left temporal bone and its pneumatisation in superior (e) and lateral views (f), and variation in the cranial vault thickness and in the thickness of the inner table, diploe and outer table (in mm) along the mid-sagittal plane (g).

Even if the petrous apex is incomplete, it is clear that cells do not propagate in this area. The most lateral and posterior extension of the pneumatisation corresponds to the cells which are located in the upper and posterior part of the petrous, at its junction with the squamous temporal.

Inferiorly, pneumatisation continues in the medial part of the mastoid process and extends under the level of the deepest point of the digastric groove. Pneumatisation has a volume of 4.4 cm^3, but this value is slightly affected by the incomplete preservation of the pneumatised areas.

The frontal bone is composed of several fragments, with plaster to complete the missing areas, particularly along the mid-sagittal plane. For this reason, the vault thickness and the internal composition were quantifiable only for the posterior third of this bone. The cranial vault thickness was quantifiable all along the junction of the parietal bones, for the occipital plane and the first half of the nuchal plane (Figure 2g). The sagittal suture extends in the analysed plane, affecting some measurements of the vault thickness and preventing the possibility of quantifying the internal composition at the junction of the parietal bones.

The thickness of the frontal bones varies from 5.1 mm for its most anterior preserved part, to 7.1 mm at the bregma. The thickness varies between 6.5 mm and 8.2 mm at the junction of the parietal bone due to the presence of the sagittal suture. There is a thickening in the anterior part of the occipital plane, from 7.5 mm at the lambda to a maximal value of 10.6 mm in the middle of the occipital plane. Then, the thickness decreases posteriorly to reach a minimal value of 9 mm, and increases again to 12 mm as a maximal value where the occipital superstructures are the most developed. The superior limit of the suprainiac fossa corresponds to a slight diminution in total thickness in comparison to the superior part of the occipital plane. Thickness increases regularly from the inferior part of the fossa towards the occipital torus. This augmentation is principally due to the presence of the internal occipital crest which becomes more developed while getting closer to the area of the endinion.

Similarly, the values for the thickness of the nuchal plane are even higher, with values around 13 mm on account of the internal occipital crest. For the internal composition (Figure 2g), the tabular tables are well represented in the most anteriorly preserved part of the frontal squama, and less close to the bregma, whereas the proportion for the diploic layer increases. Indeed, the internal table varies from 35.3 % to 23 %, the external table varies from 35.3 % to 29.7 % and the diploic layer varies from 29.4 % to 47.3 %. This variation is concomitant with the augmentation of the total vault thickness in this area. This thickening is only due to the augmentation of the thickness of the diploic layer, whereas the tabular tables do not vary to a great extent in their absolute thickness.

In the area of the occipital plane, the diploic layer is the principal constituent of the total thickness. For the area localised above the suprainiac fossa, the diploic layer has a mean representation of 64 % of the total thickness, the external table has a mean of 17 % and the internal table has a mean of 19 %. From just above the suprainiac fossa to the most posterior prominent point of the occipital torus, the mean values are 52 % for the diploic layer, 13 % for the external table and 26 % for the internal table. For the thickness quantification corresponding to the suprainiac fossa, the diploic layer has a thickness of approximately 4.8 mm, the external table is around 2.3 mm, and the internal table is about 2.6 mm. The diploic layer has a thickness of around 6.5 mm, the external table is about 3 mm, and the internal table is about 2.4 mm where the occipital superstructures are the most developed. For the preserved part of the nuchal plane, the diploic layer constitutes around 70 % of the total thickness, the internal table constitutes 13 % and the external table holds 17 %. This contribution of the diploic layer is due to the important development of the internal occipital crest in this area, whereas the external table is thinner than in the occipital superstructures.

DISCUSSION

Spy 1 and Spy 10 share similar characteristics for the extension of the frontal sinuses. These cavities completely fill the glabellar region in both individuals. Cells extend laterally as far as the middle of the frontal torus, just near the area where this structure becomes thinner vertically. In Spy 1, the cavities extend posteriorly in the area of the postorbital sulcus and slightly in the frontal squama. According to previous works, Neandertals are characterised by very large frontal sinuses, which constantly invade the frontal torus (Sergi, 1948; Vlček, 1967; Tillier, 1977). Moreover, the large development and the homogeneity of the frontal sinuses among Neandertal individuals are proposed to be autapomorphic features for this group (Tillier, 1988; Trinkaus, 1988).

Some studies have advanced a quantification of the volume of frontal sinuses. In Guattari 1, the left cavity has a volume of 3.55 cm^3 and the right one is 5.35 cm^3 (Macchiarelli, pers. comm.). Moreover, the volume of the left cavity in La Chapelle-aux-Saints 1 has a minimal value of 5.6 cm^3 and the right one is 6.3 cm^3 (Balzeau, 2005) because the frontal sinuses are not completely preserved. Similarly, the value for La Ferrassie 1 is over 12.2 cm^3 as the total for both sides. In La Quina 5, a minimal value of 3.8 cm^3 was estimated for the right side, whereas the volume for the left side was well over 2.9 cm^3. In Krapina 3, the right frontal sinus has a volume of 4.3 cm^3 and the left one is 6.8 cm^3. In Krapina 6, the frontal pneumatisation has a total volume of 10.2 cm^3 (Balzeau, 2005). In comparison, the frontal pneumatisation is not always present in *Homo erectus* from Zhoukoudian, Ngandong and Sambungmacan. If present, it constitutes a small volume and it is restricted to the glabellar region (Balzeau, 2005).

The frontal sinuses have a wide morphological and dimensional variability in adult modern humans (e.g. Weidenreich, 1934; Tillier, 1977; Szilvassy, 1982; Prossinger, 2001). In Afalou Bou Rhummel and Taforalt anatomically modern *Homo sapiens*, the morphological variation is also important and the volume of pneumatisation varies from a value of 0 to 12 cm^3 (Balzeau & Badawi-Fayad, 2005). Thus, disposition and extension of the frontal sinuses in Spy 1 and 10 are similar to the characteristics observed in other Neandertals. In these individuals, the frontal pneumatisation is always well marked, and presents some unique characteristics com-

pared to *Homo erectus* and *Homo sapiens*. The cavities invade the glabellar area and propagate laterally on a large extension into the frontal torus. Numerous cells are individualised, particularly in the uppermost and lateral extensions of the pneumatisation. Finally, pneumatisation sometimes extends in the frontal squama. However, this phenomenon is quite rare and limited because of the importance of the available areas for pneumatisation during growth into the frontal torus.

For the temporal bone pneumatisation, Australopithecines and *Paranthropus* (e.g. Kimbel & Johanson, 1984; White *et al.*, 1994; Ward *et al.*, 1999; Sherwood *et al.*, 2002) share the ape-like pattern of pneumatisation which extends throughout the entire temporal bone. There is a reduction in pneumatisation with the appearance of the genus *Homo* (Sherwood *et al.*, 2002). However, the Zhoukoudian *Homo erectus* exhibits an extensive distribution of pneumatisation through the whole temporal bone with some individual variation (Balzeau & Grimaud-Hervé, 2006). In the Ngandong and Sambungmacan *Homo erectus*, pneumatisation is restricted mainly to the area inferior to the supramastoid crest and anterior to the mastoid crest, as well as to the lateral part of the petrous temporal (Balzeau & Grimaud-Hervé, 2006). Finally, the pneumatisation expansion in modern humans is generally limited to the mastoid, perilabyrinthine and petrous regions, whereas extension into the squamous temporal is rare and not extensive (e.g. Turner & Porter, 1922; Allam, 1969; Wolfowitz, 1974; Schulter, 1976; Virapongse *et al.*, 1985; Zonneveld, 1987; Scheuer & Black, 2000; Koç *et al.*, 2004).

The data for Spy 1 and 10 totally match the Neandertal adult pattern for temporal bone pneumatisation described previously (Balzeau & Radovčić, 2008). Spy 1 has the most important asymmetry for temporal bone pneumatisation, based on the available data for Neandertals. The intra-individual variation in the volume of Spy 1 (1.1 cm^3 for the left side and 4.8 cm^3 for the right side) is quite important compared to the inter-individual variation in Neandertals (from 1.1 cm^3 to more than 5 cm^3 and a mean value of 2.39 cm^3 with SD = 1.03 cm^3 and N = 14). Nevertheless, the disposition of pneumatisation on both sides remains typical for Neandertals. Moreover, this variation does not differ from asymmetries observable in modern humans when "normal" variation is considered in large samples (e.g. Virapongse *et al.*, 1985; Koç *et al.*, 2003; Lee *et al.*, 2005).

In sum, Neandertals share a reduced asymmetry of temporal bone pneumatisation with the *Homo erectus* individuals from Ngandong and Sambungmacan (Balzeau & Grimaud-Hervé, 2006) and modern humans (e.g. Virapongse *et al.*, 1985; Lee *et al.*, 2005). Moreover, Neandertals show a pattern for pneumatisation with a lower degree of variation than modern humans, and with a slightly lower extension into the different areas of the temporal bone than *Homo erectus* and *Homo sapiens* (Balzeau & Radovčić, 2008).

The available data for cranial vault thickness and internal composition concern "classic" Neandertals (Balzeau, 2005) and individuals from Krapina (Balzeau, 2007). La Chapelle-aux-Saints 1, La Ferrassie 1, La Quina 5 and Spy 1 are preserved for nearly the full extension of their mid-sagittal plane. Krapina 3, 4 and 6 provide data for the frontal bone. Spy 10 and Krapina 5 comprise relatively well-preserved parietal and occipital bones. These individuals show some variability in terms of thickness, but maintain a similar pattern of distribution of the cranial vault thickness along the mid-sagittal plane (Figures 1 and 2; Balzeau, 2005, 2007).

Thickness decreases rapidly and regularly from the area of the frontal torus to the middle part of the frontal squama. The variation along the junction of the parietal bones shares similar characteristics. On the occipital bone, an increase of the thickness is visible in the middle part of the occipital squama. The suprainiac fossa only induces a reduced variation in CVT and is not responsible for the decrease in thickness between the middle part of the occipital squama and the occipital superstructures.

Finally, Neandertals show a limited increase of thickness in the direction of the external occipital protuberance and are unique for the variation in thickness in the area of the occipital superstructures as compared to *Homo erectus* and anatomically modern *Homo sapiens* (Balzeau, 2006). For the internal composition, all the analysed Neandertals share similar characteristics.

The diploic layer is the principal constituent of the frontal and occipital bones in the mid-sagittal plane. Moreover, the occipital superstructures do not correspond to a unique thickening of the external table. It is principally the diploic layer which is affected by the variations in total thickness of the occipital bone. For these aspects, Neandertals differ from *Homo erectus* and *Homo sapiens* (Balzeau, 2006).

These data also highlight the ambiguous relation between cranial vault thickness and sexual attribution of Neandertal specimens. For example, Spy 10 (presumably a male) has values for CVT that are below those of Spy 1, which is presumably a female, for most of the analysed landmarks. Consequently, CVT along the mid-sagittal plane, which includes the frontal and occipital superstructures, does not appear to be a discriminating indicator of sexual determination in Neandertals. CVT seems to be influenced by a size and robustness component. This set of correlated features is probably more meaningful for clarifying sexual attribution when the extreme individuals of the variation are considered.

CONCLUSIONS

We are now able to deepen our knowledge of the morphology of fossils by getting access to previously unavailable features thanks to imaging methodologies. This approach also allows one to identify new characteristics to debate the morphological variation among hominid species, as well as their relationships. This paper provides exhaustive descriptions and detailed metric data for the pneumatisation of the frontal and temporal bones and for the cranial vault thickness and its internal composition for the Spy 1 and Spy 10 crania. These two individuals fall within the morphological variation observed among Neandertals for the analysed features. Finally, as described above, this fossil group has some typical features for the pneumatisation of the frontal and temporal bones, as well as for the cranial vault thickness and its internal composition as compared to *Homo erectus* and *Homo sapiens*. Additional work is needed to better understand the variation of these features among hominids and to explore their possible phylogenetic implications further.

ACKNOWLEDGEMENTS

This research has been supported by the Royal Belgian Institute of Natural Sciences and the TNT project ("The Neanderthal Tools"), 6th Framework of the European Community. I am very thankful to the following individuals for access to fossils in their care and for providing CT data: P. Semal, Scientific Heritage & Earth and History of Life, Royal Belgian Institute of Natural Sciences, Brussels, Belgium; J. Radovčić, Department of Geology and Palaeontology, Croatian Natural History Museum, Zagreb, Croatia; S. Bahuchet and P. Mennecier, *Département Hommes, Natures, Sociétés, Muséum national d'Histoire naturelle*, Paris, France; H. de Lumley and F. Sémah, *Département de Préhistoire, Muséum national d'Histoire naturelle*, Paris, France. I thank E. A. Cabanis and J. Badawi-Fayad –*CHNO des Quinze-Vingts*, Paris– for the scanning procedures in Paris, and the Department of Radiology, University of Zagreb, hospital *Bolnica Sestara Milosrdnica*, Zagreb, for the scanning procedures on the Krapina fossils. I am grateful to the technical partner (Art+com) of the TNT project for the collaborative development of the ArteCore software.

BIBLIOGRAPHY

ALLAM A. F., 1969. Pneumatization of the temporal bone. *Annals of Otology, Rhinology and Laryngology*, **78**: 49-64.

BALZEAU A., 2005. *Spécificités des caractères morphologiques internes du squelette céphalique chez* Homo erectus. Thèse de doctorat, Muséum National d'Histoire Naturelle, Paris.

BALZEAU A., 2006. Are thickened cranial bones and equal participation of the three structural bone layers autapomorphic traits of *Homo erectus*? *Bulletins et Mémoires de la Société d'Anthropologie de Paris*, **18**: 145-163.

BALZEAU A., 2007. Variation and characteristics of the cranial vault thickness in Krapina and Western European Neandertals. *Periodicum Biologorum*, **109**: 369-377.

BALZEAU A. & BADAWI-FAYAD J., 2005. La morphologie externe et interne de la région supra-orbitaire est-elle corrélée à des contraintes biomécaniques? Analyses structurales des populations d'*Homo sapiens* d'Afalou Bou Rhummel (Algérie) et de Taforalt (Maroc). *Bulletins et Mémoires de la Société d'Anthropologie de Paris*, **17**: 185-197.

BALZEAU A. & GRIMAUD-HERVÉ D., 2006. Cranial base morphology and temporal bone pneumatization in Asian *Homo erectus*. *Journal of Human Evolution*, **51** (4): 350-359.

BALZEAU A., GRIMAUD-HERVÉ D. & JACOB T., 2005. Internal cranial features of the Mojokerto child fossil (East Java, Indonesia). *Journal of Human Evolution*, **48** (6): 535-553.

BALZEAU A., INDRIATI E., GRIMAUD-HERVÉ D. & JACOB T., 2003. Computer tomography scanning of *Homo erectus* crania Ngandong 7 from Java: Internal structure, paleopathology and post-mortem history. *Berkala Ilmu Kedokteran (Journal of the Medical Sciences)*, **35**: 133-140.

BALZEAU A. & RADOVČIĆ J., 2008. Variation and modalities of growth and development of the temporal bone pneumatization in Neandertals. *Journal of Human Evolution*, **54** (5): 546-567.

KIMBEL W. H. & JOHANSON D. C., 1984. Cranial morphology of *Australopithecus afarensis*: a comparative study based on a composite reconstruction of the adult skull. *American Journal of Physical Anthropology*, **64** (4): 337-388.

KOÇ A., EKINCI G., BILGILI A. M., AKPINAR I. N., YAKUT H. & HAN T., 2003. Evaluation of the mastoid air cell system by high resolution computed tomography: three-dimensional multiplanar volume rendering technique. *Journal of Laryngology & Otology*, **117**: 595-598.

KOÇ A., KARAASLAN O. & KOÇ T., 2004. Mastoid air cell system. *Otoscope*, **4**: 144-154.

LEE D. H., JUN B. C., KIM D. G., JUNG M. K. & YEO S. W., 2005. Volume variation of mastoid pneumatization in different age groups: a study by three-dimensional reconstruction based on computed tomography images. *Surgical and Radiologic Anatomy*, **24**: 37-42.

MACCHIARELLI R., RADOVČIĆ J., SEMAL P. & WENIGER G. C., 2005. A "virtual reality" for the Neanderthal fossil record: "The Neanderthal Tools" project. *Bulletins et Mémoires de la Société d'Anthropologie de Paris*, **17**: 14.

MACCHIARELLI R. & WENIGER G. C., 2006. NESPOS: from data accumulation to data management. Abstracts of the congress '150 years of Neanderthals discoveries, continuity and discontinuity', Bonn, Germany. *Terra Nostra*, **2**: 83-84.

PROSSINGER H., 2001. Sexually dimorphic ontogenetic trajectories of frontal sinus cross section. *Collegium antropologicum*, **25**: 1-11.

SCHEUER L. & BLACK S., 2000. *Developmental Juvenile Osteology*. London, Elsevier Academic Press.

SCHULTER F. P., 1976. A comparative study of the temporal bone in three populations of man. *American Journal of Physical Anthropology*, **44** (3): 453-468.

SCHWARTZ G. T., THACKERAY J. F., REID C. & VAN REENAN J. F., 1998. Enamel thickness and the topography of the enamel-dentine junction in South African Plio-Pleistocene hominids with special reference to the Carabelli trait. *Journal of Human Evolution*, **35** (4-5): 523-542.

SEMAL P., TOUSSAINT M., MAUREILLE B., ROUGIER H., CREVECOEUR I., BALZEAU A., BOUCHNEB L., LOURYAN S., DE CLERCK N. & RAUSIN L., 2005. Numérisation des restes hu-

mains néandertaliens belges. Préservation patrimoniale et exploitation scientifique. *Notae Praehistoricae*, **25**: 25-38.

SERGI S., 1948. Sulla morfologia della facies anterior corporis maxillae nei Paleantropi di Saccopastore e del Monte Circeo. *Atti dell'Accademia Nazionale dei Lincei*, **8**: 387-394.

SHERWOOD R. J., WARD S. C. & HILL A., 2002. The taxonomic status of the Chemeron temporal (KNM-BC 1). *Journal of Human Evolution*, **42** (1-2): 153-184.

SPOOR C. F., ZONNEVELD F. & MACHO G., 1993. Linear measurements of cortical bone and dental enamel by computed tomography: applications and problems. *American Journal of Physical Anthropology*, **91** (4): 469-484.

SZILVASSY J., 1982. Zur Variation Entwicklung und Vererbung der Stirnhohlen. *Annalen des Naturhistorischen Museums in Wien*, **1**: 97-125.

TILLIER A.-M., 1977. La pneumatisation du massif cranio-facial chez les hommes actuels et fossiles. *Bulletins et Mémoires de la Société d'Anthropologie de Paris*, **13**: 177-189, 287-316.

TILLIER A.-M., 1988. À propos des séquences phylogénétiques et ontogénétiques chez les Néanderthaliens. *In*: E. TRINKAUS (ed.), *L'Homme de Néandertal, 3. L'Anatomie*. Liège, ERAUL: 125-135.

TRINKAUS E., 1988. The evolutionary origins of the Neandertals or why were there Neandertals? *In*: E. TRINKAUS (ed.), *L'Homme de Néandertal, 3. L'Anatomie*. Liège, ERAUL: 11-29.

TURNER A. & PORTER W. A., 1922. The structural type of the mastoid process based upon the skiagraphic examination of 1000 crania of various races of mankind. *Journal of Laryngology & Otology*, **37**: 115-121.

VIRAPONGSE C., SARWAR M., BHIMANI S., SASAKI C. & SHAPIRO R., 1985. Computed tomography of temporal bone pneumatization: 1. Normal pattern and morphology. *American Journal of Roentgenology*, **147**: 473-481.

VLČEK E., 1967. Die sinus frontales bei europäischen Neanderthalern. *Anthropologischer Anzeiger*, **30**: 166-189.

WARD C. V., LEAKEY M. & WALKER A., 1999. The new hominid species *Australopithecus anamensis*. *Evolutionary Anthropology*, **7**: 197-205.

WEIDENREICH F., 1934. Das Menschenkinn und seine Entstehung. *Ergebnisse der Anatomie und Entwicklungsgeschichte*, **31**: 1-124.

WHITE T. D., SUWA G. & ASFAW B., 1994. *Australopithecus ramidus*, a new species of early hominid from Aramis, Ethiopia. *Nature*, **371**: 306-312.

WOLFOWITZ B. L., 1974. *Pneumatization of the skull of the South African negro*. Ph.D. Dissertation, University of the Witwatersrand, Johannesburg, South Africa.

ZONNEVELD F., 1987. *Computed Tomography of the temporal bone and orbit*. Munich, Urban & Schwarzenberg.

AUTHOR'S AFFILIATION

Antoine BALZEAU
CNRS
Équipe de Paléontologie Humaine
UMR 7194
Département de Préhistoire
du Muséum national d'Histoire naturelle
Musée de l'Homme
17, place du Trocadéro
75016 Paris
France
abalzeau@mnhn.fr
and
Earth and History of Life
Royal Belgian Institute of Natural Sciences
29, Vautier Street
1000 Brussels
Belgium